biomedicines

MDPI

Article

Netrin-4 Is Induced After Intervertebral Disc Injury, and Exposure to Recombinant Netrin-4 Is Associated with Inflammatory and Catabolic Gene Expression Changes in Cultured Mouse Disc Cells

Naoya Shibata [1], Kentaro Uchida [1,2,*], Masayuki Miyagi [1], Gen Inoue [1], Yusuke Mimura [1], Yuji Yokozeki [1], Yui Uekusa [1], Yuki Jojo [3] and Masashi Takaso [1]

[1] Department of Orthopaedic Surgery, Kitasato University School of Medicine, 1-15-1 Minami-ku, Kitasato, Sagamihara 252-0374, Kanagawa, Japan; shibata.naoya@st.kitasato-u.ac.jp (N.S.); masayuki008@gmail.com (M.M.); ginoue@kitasato-u.ac.jp (G.I.); mimura.yusuke@st.kitasato-u.ac.jp (Y.M.); yuji0328yoko@yahoo.co.jp (Y.Y.); uekusa.yui@st.kitasato-u.ac.jp (Y.U.); mtakaso@kitasato-u.ac.jp (M.T.)
[2] Research Institute, Shonan University of Medical Sciences, Nishikubo 500, Chigasaki 253-0083, Kanagawa, Japan
[3] Department of Medical Engineering and Technology, Graduate School of Medical Sciences, Kitasato University, 1-15-1 Minami-ku, Kitasato, Sagamihara 252-0375, Kanagawa, Japan; jojo.yuki@st.kitasato-u.ac.jp
* Correspondence: kuchida@med.kitasato-u.ac.jp; Tel.: +81-42-778-9217

Abstract

Background/Objectives: Intervertebral disc (IVD) injury induces inflammatory and extracellular matrix (ECM) remodeling responses that may contribute to disc degeneration. However, the role of netrin-4 (NTN4) in these responses remains unclear. This study investigated NTN4 expression after IVD injury and cellular responses to recombinant NTN4 exposure in cultured mouse IVD cells. **Methods**: Male C57BL/6J mice underwent coccygeal disc puncture, and the expression of *Ntn4*, its putative receptor genes *Unc5b* and *Neo1*, and matrix- and inflammation-related genes was assessed in IVD tissues at baseline and on days 7, 14, and 28 after injury. Immunoreactive bands detected using antibodies against NTN4, NEO1, and UNC5B were examined by Western blotting, and immunoreactivity detected using the anti-NTN4 antibody was evaluated by immunohistochemistry at baseline (day 0) and on day 14 after injury. Cultured mouse IVD cells were treated with recombinant NTN4 at 0, 50, or 500 ng/mL, and gene expression, receptor antibody-reactive band intensities, and culture supernatant protein concentrations were analyzed using quantitative reverse transcription polymerase chain reaction, Western blotting, and ELISA, respectively. **Results:** *Ntn4* mRNA expression decreased on day 7 and increased on days 14 and 28, whereas *Neo1* expression increased on day 14 and *Unc5b* expression showed no significant change at this time point. Comparison of uninjured and day 14 post-injury tissues showed increased intensities of NTN4-, NEO1-, and UNC5B-immunoreactive bands after injury. Immunohistochemistry revealed NTN4 immunoreactivity in cells located within the nucleus pulposus region of the injured IVD. At 24 h, cells exposed to the tested recombinant NTN4 preparation at 500 ng/mL showed higher *Il6*, *Tnf*, *Mmp3*, and *Mmp13* expression and lower *Col2a1* and *Acan* expression than controls. At 50 ng/mL, *Il6* and *Mmp13* expression was significantly higher at both 6 and 24 h, whereas *Mmp3* expression and culture supernatant IL-6 concentrations were significantly higher at 24 h compared with the corresponding controls. At 500 ng/mL, culture supernatant concentrations of IL-6, MMP-3, and MMP-13 were also higher than in controls. **Conclusions**: These findings indicate increased *Ntn4* mRNA expression and anti-NTN4 immunoreactive band intensity following IVD injury. However, the observed cellular responses to the recombinant NTN4 preparation cannot be

Check for updates

Academic Editors: Elisa Belluzzi and Assunta Pozzuoli

Received: 25 September 2026
Revised: 16 November 2026
Accepted: 16 November 2026
Published: 18 November 2026

Copyright: © 2026 by the authors. Licensee MDPI, Basel, Switzerland. This article is an open access article distributed under the terms and conditions of the Creative Commons Attribution (CC BY) license.

attributed specifically to NTN4, and the causal role of endogenous NTN4 in post-injury inflammatory and catabolic responses remains unclear. Further studies are needed to clarify the biological role of NTN4 following IVD injury.

Keywords: Netrin-4; intervertebral disc; inflammation; matrix metabolism

1. Introduction

Intervertebral disc (IVD) degeneration is a major pathological condition associated with low back pain, functional impairment, and reduced quality of life [1]. The IVD consists of the nucleus pulposus, annulus fibrosus, and cartilaginous endplate, which together maintain spinal flexibility and resistance to mechanical loading [2,3]. Disc degeneration is characterized by progressive loss of proteoglycans, disorganization of collagen networks, alterations in cellular phenotype, and impaired biomechanical function [4,5]. Although aging and repetitive mechanical stress contribute to IVD degeneration, direct injury to the IVD can initiate or accelerate degenerative changes through inflammation, cellular stress, and disruption of extracellular matrix (ECM) homeostasis [6].

The maintenance of IVD structure depends on a balance between ECM synthesis and degradation. Following disc injury, matrix turnover is increased, and inflammatory cytokines such as tumor necrosis factor-alpha (TNF-α), interleukin-1beta (IL-1β), and interleukin-6 (IL-6) can promote a catabolic microenvironment in disc cells [7,8]. Excessive expression of matrix-degrading enzymes can further promote progressive tissue degeneration. Matrix metalloproteinase (MMP)-3 and MMP-13 are involved in the degradation of proteoglycans and collagens and have been implicated in the pathogenesis of IVD degeneration [9–11]. Therefore, identifying molecular factors that regulate inflammatory responses and matrix remodeling may improve the understanding of the biological response of the IVD to injury.

Netrins are a family of secreted laminin-related proteins originally identified as axon guidance molecules during neural development [12]. In addition to their roles in the nervous system, netrins regulate cell adhesion, migration, angiogenesis, inflammation, tissue integrity, and repair through interactions with receptors such as deleted in colorectal cancer (DCC), neogenin (NEO1), and UNC5 family members [12–14]. Netrin-1 has also been implicated in chondrogenic and osteogenic differentiation, suggesting a potential relationship between netrin signaling and skeletal or cartilage-related cell biology [15]. Among the netrin family, Netrin-1 has been most extensively studied in IVD pathology. Previous studies have reported increased Netrin-1 expression in degenerated human discs and have suggested that Netrin-1 contributes to nerve ingrowth, angiogenesis, and discogenic pain [16,17]. These findings indicate that netrin signaling may be relevant to the pathological microenvironment of the injured and degenerated IVD.

Netrin-4 (NTN4) has biological properties distinct from those of netrin-1, including interactions with laminin networks that regulate basement membrane organization [13,18,19]. NTN4 has also been reported to interact with NEO1 and Unc-5 netrin receptor B (UNC5B) and to regulate angiogenesis, endothelial responses, inflammation, and tissue stability in a context-dependent manner [13,20]. In addition, NTN4 has been implicated in epithelial and nerve regeneration during corneal wound healing and is upregulated in a rat model of rotator cuff tear, suggesting that NTN4 may be induced in response to tissue injury and may participate in local tissue remodeling [21,22]. NTN4 expression has also been examined in osteoarthritis-related tissues, including synovium and infrapatellar fat pad, where it was associated with inflammatory, stromal, or sensory

neuron-related responses [23,24]. However, whether Ntn4 expression changes after IVD injury and how cultured disc cells respond to recombinant NTN4 exposure remain unclear.

In the present study, we investigated the temporal expression of *Ntn4* and its putative receptor genes, *Neo1* and *Unc5b*, together with ECM, MMP, and inflammatory cytokine genes, in a mouse model of IVD injury. We also examined NTN4-, NEO1-, and UNC5B-immunoreactive band intensities by Western blotting and anti-NTN4 immunoreactivity in disc tissue. Finally, we evaluated gene expression and protein concentrations in culture supernatants of mouse IVD cells following exposure to recombinant NTN4.

2. Materials and Methods

2.1. Experimental Animals and Study Design

A total of 86 male C57BL/6J mice (nine weeks old; Charles River Laboratories, Yokohama, Japan) were used: 40 for in vivo gene expression analysis, 16 for Western blot analysis, 10 for histological analysis ($n = 5$ per group), and 20 for in vitro experiments. All mice were wild-type C57BL/6J mice and had not undergone any experimental procedures before study entry. Mice were housed under a semi-barrier system at 23 ± 2 °C and 55 ± 10% humidity with a 12 h light/dark cycle and free access to commercial chow (CRF-1; Oriental Yeast Industry, Tokyo, Japan) and water. All procedures were conducted in accordance with the Science Council of Japan's guidelines and approved by the Kitasato University Animal Ethics Committee (approval no. 2026-006).

For in vivo gene expression analysis, 40 mice were divided into four groups ($n = 10$ per group): an intact control group (day 0) and groups evaluated at 7, 14, and 28 days after IVD injury. Intact control mice did not undergo surgery or disc puncture. Mice were nine weeks old upon arrival and were acclimatized for at least one week before the experiments. The mice were 10 weeks old at the time of surgery. Tissue collection was performed at 10 weeks of age for the intact control group (day 0) and at 11, 12, and 14 weeks of age for the day 7, 14, and 28 post-injury groups, respectively. In the injury groups, anesthesia was induced with isoflurane (Viatris Healthcare G.K., Tokyo, Japan), followed by an intramuscular injection of a 1:3:1 anesthetic mixture containing midazolam (Product no. KB6762; Sando, Yamagata, Japan), medetomidine hydrochloride (Domitor; Product no. 005130; Orion Corporation, Espoo, Finland), and butorphanol tartrate (Vetorphale; Product no. VETLI5; Meiji Seika Pharma Co., Ltd., Tokyo, Japan) at a dose of 0.05 mL/100 g body weight. Six consecutive coccygeal IVDs, starting at the Co5/6 level, were injured by percutaneous puncture using a 27-gauge needle, based on a previously reported mouse IVD injury model [25,26]. Mice were placed in the prone position, and the needle was inserted vertically through the dorsal skin into each IVD. Each disc was punctured 10 times through the same entry site without traversing the entire disc. Needle insertion depth was not quantitatively controlled using a predetermined depth or mechanical stop. Six consecutive disc levels were selected to obtain sufficient tissue for molecular analyses.

For gene expression and Western blot analyses, IVD tissues containing the nucleus pulposus and annulus fibrosus were carefully dissected under a stereomicroscope, excluding the cartilaginous endplate, growth plate, vertebral bone, and bone marrow. The six IVDs collected from each mouse were pooled to generate a single biological sample for each assay, with the individual mouse serving as the experimental unit. IVD tissues were collected at the indicated time points for gene expression analysis. The nucleus pulposus and annulus fibrosus were harvested together and were not analyzed separately. For Western blot analysis, IVD tissues were collected from 16 additional mice: intact controls and mice at 14 days after injury ($n = 8$ per group). For histological analysis, IVD tissues were collected from 10 additional mice: five intact controls (day 0) and five mice at 14 days after injury. For in vitro experiments, 20 additional intact mice were used in four independent experi-

ments, with five mice used for each cell isolation, as described in Section 2.5. Mice were allowed to acclimatize to the animal facility for at least 1 week before experiments. Standard bedding and environmental enrichment were provided according to institutional animal facility procedures.

The primary in vivo outcome was *Ntn4* mRNA expression after IVD injury. Secondary outcomes included *Unc5b* and *Neo1* mRNA expression, extracellular matrix-, MMP-, and inflammatory cytokine-related gene expression, all assessed by qPCR, as well as anti-NTN4 antibody-reactive band intensity assessed by Western blotting and the distribution of anti-NTN4 immunoreactivity assessed by immunohistochemistry.

For in vivo gene expression and Western blotting analyses, the experimental unit was the individual mouse. For histological analysis, representative IVD sections from each mouse were evaluated. For in vitro experiments, the experimental unit was an independent cell isolation prepared from five mice. Each isolation contributed one well per treatment condition and time point for qPCR analysis, with culture supernatants collected from the same wells at 24 h for ELISA before RNA extraction. Separate wells prepared in parallel using cells from the same isolations and exposed to the same NTN4 concentrations for 24 h were used for Western blot analysis. All in vitro analyses were based on four independent cell isolations ($n = 4$ biological replicates), and no technical replicate wells were averaged within each assay.

Sample sizes were determined based on previous mouse IVD injury studies, prior laboratory experience with qPCR and Western blot analyses, and the principle of using the minimum number of animals required to obtain interpretable data. No formal a priori sample size calculation was performed.

Inclusion criteria were healthy male C57BL/6J mice at nine weeks of age. No additional exclusion criteria were established a priori. No animals, experimental units, or data points were excluded from the analyses.

Animals were allocated to the in vivo gene expression, Western blotting, histological, and in vitro experiments before tissue collection. For the time-course injury experiment, formal randomization was not performed because groups were defined by the sampling time after injury and the day 0 group consisted of intact controls. Potential confounding was minimized by using male mice of the same strain and age, performing procedures under standardized conditions, and processing samples according to predefined protocols.

Investigators were not blinded to group allocation during the surgical procedures or tissue collection. Quantitative outcome measurements were performed using predefined experimental and statistical procedures, and group labels were retained during data analysis.

After IVD injury, mice were monitored daily for general condition, posture, activity, wound condition, and signs of pain or distress. Humane endpoints were defined as severe distress, inability to access food or water, marked impairment of ambulation, wound infection, or body weight loss exceeding 20%. No unexpected adverse events or deaths before the scheduled endpoints were observed. At each endpoint, mice were euthanized by CO_2 inhalation before tissue collection, in accordance with institutional procedures.

2.2. Quantitative Polymerase Chain Reaction

Immediately after collection, IVD tissues were homogenized in TRIzol reagent (Product no. 15596026; Invitrogen, Carlsbad, CA, USA) on ice. Total RNA was purified using the Direct-zol RNA MicroPrep kit (Zymo Research, Irvine, CA, USA), including on-column DNase I treatment, according to the manufacturer's instructions. RNA purity was assessed using the A260/A280 absorbance ratio, with values ranging from 1.8 to 2.0. Purified RNA was reverse transcribed into complementary DNA (cDNA) using SuperScript III Reverse Transcriptase (Product no. 18080085; Invitrogen).

Each quantitative polymerase chain reaction (qPCR) was performed in a total volume of 25 µL containing 2 µL of cDNA template, gene-specific forward and reverse primers at a final concentration of 0.2 µM each, and 12.5 µL of SYBR Premix Ex Taq (Product no. RR820; Kusatsu, Shiga, Japan). The primer sequences are listed in Table 1.

Table 1. Primer sequences used in this study.

Gene		Sequence	bp
Acan	sense	CAGATGGCACCCTCCGATAC	151
	antisense	GACACACCTCGGAAGCAGAA	
Col2a1	sense	GGAGAGACCATGAACGGTGG	78
	antisense	CATCTGGACGTTAGCGGTGT	
Il6	sense	CTGCAAGAGACTTCCATCCAG	131
	antisense	AGTGGTATAGACAGGTCTGTTGG	
Mmp3	sense	GTCCTCCACAGACTTGTCCC	102
	antisense	AGGACATCAGGGGATGCTGT	
Mmp13	sense	ATGAACATCCATCCCGTGACC	170
	antisense	GGTCTTCCCCGTGTTCTCAAA	
Neo1	sense	TCCTGCTCCAGTTGTTAGATGG	197
	antisense	GTGGCACTTGCACAGTAAGC	
Ntn4	sense	GCAACAAACTGCTCGGCTAC	138
	antisense	GTCGTATGGTGGTGACAGGG	
Tnf	sense	CTGAACTTCGGGGTGATCGG	122
	antisense	GGCTTGTCACTCGAATTTTGAGA	
Unc5b	sense	GACCACGTCACACAGGAGAG	160
	antisense	GGCGACTCTTGGTAGTTCCC	
Gapdh	sense	AACTTTGGCATTGTGGAAGG	223
	antisense	ACACATTGGGGGTAGGAACA	

qPCR was conducted using a CFX96 Real-Time PCR Detection System (Bio-Rad, Hercules, CA, USA). The amplification protocol consisted of an initial denaturation step at 95 °C for 1 min, followed by 40 cycles of denaturation at 95 °C for 5 s and annealing/extension at 60 °C for 30 s. The specificity of qPCR amplification was assessed by melting curve analysis.

Gapdh was used as the internal reference gene. For each sample, ΔCt values were calculated by subtracting the Ct value of *Gapdh* from that of the target gene, and relative expression levels were calculated as $2^{-\Delta Ct}$. For in vivo analyses, these values were normalized to the arithmetic mean of the relative expression values from the intact control group (day 0). For in vitro analyses, normalization was performed separately for each gene and treatment time point using the arithmetic mean of the relative expression values from the four independent control samples (0 ng/mL NTN4). Thus, the mean relative expression of each control group was set to 1, while variability among individual control samples was retained. The raw Cq values for the in vivo and in vitro qPCR analyses are provided in Supplementary Tables S1 and S3, respectively.

2.3. Western Blotting

Proteins were extracted from IVD tissues collected from intact controls and mice at 14 days after injury ($n = 8$ per group) using a sodium dodecyl sulfate (SDS)-containing extraction buffer. Protein concentrations were determined using a Pierce BCA Protein Assay Kit (Thermo Fisher Scientific, Rockford, IL, USA). Equal amounts of protein (5 µg/lane) were separated by SDS–polyacrylamide gel electrophoresis using 5–20% gradient gels (ePAGEL; ATTO, Tokyo, Japan) at a constant current of 10 mA for 30 min, followed by 20 mA for 60 min and transferred onto polyvinylidene difluoride membranes (Millipore,

Burlington, MA, USA) at 12 V and 400 mA for 60 min. A prestained protein molecular weight marker (WIDE-VIEW™ Prestained Protein Size Marker III; Cat. No. 230-02461; FUJIFILM Wako Pure Chemical Corporation, Osaka, Japan) was used to estimate the apparent molecular weights of the immunoreactive bands. The membranes were blocked with 5% skim milk for 30 min at room temperature and incubated overnight at 4 °C with primary antibodies against NTN4 (1:1000; bs-6711R; Bioss, Woburn, MA, USA), followed by incubation with a horseradish peroxidase (HRP)-conjugated anti-rabbit IgG secondary antibody (1:2000; FUJIFILM Wako Pure Chemical Corporation) for 1 h at room temperature. Immunoreactive bands were detected using Chemi-Lumi One (Nacalai Tesque, Kyoto, Japan) and imaged using a FUSION imaging system (Vilber Bio Imaging, Collégien, France) with exposure times of 20 s for IVD tissue samples. After NTN4 detection, the membranes were treated with WB Stripping Solution (Nacalai Tesque) for 15 min at room temperature with gentle agitation to remove bound antibodies. The membranes were then washed with Tris-buffered saline containing Tween 20 (TBST), reblocked, and incubated overnight at 4 °C with a mouse monoclonal anti-GAPDH antibody (1:1000; 014-25524; FUJIFILM Wako Pure Chemical Corporation, Osaka, Japan), followed by incubation with an HRP-conjugated goat anti-mouse IgG (H + L) secondary antibody (1:2000; 115-035-003; Jackson ImmunoResearch Laboratories, West Grove, PA, USA) for 1 h at room temperature. GAPDH immunoreactivity was detected using Chemi-Lumi One and imaged using the same FUSION imaging system with exposure times of 10 s for IVD tissue samples.

For analysis of NTN4 receptors, equal amounts of protein (5 μg/lane) were separated using 5–20% gradient gels (ePAGEL; ATTO) at a constant current of 20 mA for 30 min, followed by 40 mA for 60 min, and transferred onto polyvinylidene difluoride membranes at 24 V for 30 min. After blocking, membranes were incubated with a rabbit monoclonal anti-UNC5B antibody (1:1000; clone EPR26173-186; ab313365; Abcam, Cambridge, UK), followed by the same HRP-conjugated anti-rabbit IgG secondary antibody used for NTN4 detection. Following detection of UNC5B, the membranes were stripped, washed with TBST, reblocked, and incubated with an anti-Neogenin antibody (1:5000; 20246-1-AP; Proteintech, Rosemont, IL, USA), followed by the same secondary antibody. After Neogenin detection, the membranes were stripped again, washed, reblocked, and incubated with the anti-GAPDH antibody for normalization. Immunoreactive bands were detected using the chemiluminescence and imaging procedures described above. Exposure times for UNC5B were 2 min 30 s (IVD tissue) and 1 min 14 s (cultured IVD cells); those for Neogenin were 15 s (IVD tissue) and 1 min 18 s (cultured IVD cells). Following the final stripping step, GAPDH was imaged with exposure times of 5 s (IVD tissue) and 15 s (cultured IVD cells).

Band intensities were quantified using BIO-1D software (Vilber Bio Imaging) from the original 16-bit grayscale images. Identically sized ROIs were applied to the approximately 63 kDa immunoreactive band and the GAPDH band across all 16 lanes. Background subtraction was performed using the rolling-ball approach implemented in BIO-1D software. The intensity of the approximately 63 kDa band detected using the anti-NTN4 antibody was normalized to that of GAPDH and expressed relative to the mean of the intact control group. For receptor analysis, the immunoreactive band at approximately 103 kDa, corresponding to the predicted molecular weight of UNC5B, was used for quantification. For Neogenin, the band at approximately 180 kDa, corresponding to the molecular weight reported by the antibody manufacturer (calculated molecular weight, 160 kDa), was quantified. An additional immunoreactive band was observed at approximately 60 kDa with the anti-Neogenin antibody but was not included in the quantification. The intensities of the selected UNC5B and Neogenin bands were normalized to the corresponding GAPDH band intensities and expressed relative to the mean of the intact control group.

2.4. Histological Analysis

IVD tissues collected from intact controls (day 0) and mice at 14 days after injury ($n = 5$ per group) were fixed in 4% paraformaldehyde in phosphate-buffered saline (Nacalai Tesque, Kyoto, Japan) for 48 h, decalcified in EDTA (FUJIFILM Wako Pure Chemical Corporation, Osaka, Japan) for 2 weeks, and embedded in paraffin. Three coccygeal IVD levels were examined per mouse, yielding a total of 30 discs (15 discs per group). Sections were cut at a thickness of 4 μm, and four sections per disc were evaluated, yielding a total of 120 sections (60 sections per group). Serial sections were used for hematoxylin and eosin (H&E) staining and NTN4 immunohistochemistry. For immunohistochemical analysis, sections were deparaffinized, and endogenous peroxidase activity was quenched with hydrogen peroxide. Antigen retrieval was not performed. Preliminary immunohistochemical staining was performed using anti-NTN4 antibody dilutions of 1:200, 1:400, 1:800, and 1:1600. Background staining was observed at dilutions of 1:200, 1:400, and 1:800 but was reduced at 1:1600. Therefore, a dilution of 1:1600 was selected for subsequent immunohistochemical analyses. The sections were incubated with an anti-NTN4 antibody (1:1600; bs-6711R; Bioss, Woburn, MA, USA) for 1 h at room temperature, followed by Histofine Simple Stain MAX-PO (R) (Nichirei Biosciences, Tokyo, Japan). Immunoreactivity was visualized using 3,3′-diaminobenzidine (DAB; Dako, Glostrup, Denmark), and the sections were counterstained with Mayer's hematoxylin. For negative controls, the primary antibody was omitted, and sections from both day 0 and day 14 were processed using the same immunohistochemical staining procedure. Histological evaluation was performed without blinding, and no formal semiquantitative histological injury or degeneration scoring was performed.

2.5. Isolation and Culture of Mouse Intervertebral Disc Cells

For each independent in vitro experiment, IVD cells were isolated from five healthy, intact mice. Six consecutive coccygeal IVDs, beginning at the Co5/6 level, were harvested from each mouse, yielding 30 discs per experiment. The collected discs were minced into small fragments and digested with 0.1% collagenase I (FUJIFILM Wako Pure Chemical Corporation) at 37 °C for 1 h. Cells obtained from all 30 discs were pooled and cultured together in a single flask in α-minimum essential medium (α-MEM; Gibco, Grand Island, NY, USA) supplemented with 10% fetal bovine serum (FBS; Gibco). Four independent experiments were performed using separate sets of five mice, for a total of 20 mice. Cells were maintained at 37 °C in a humidified atmosphere containing 5% CO_2. After 1 week, the culture medium was replaced. After approximately 2 weeks of primary culture, the cells were passaged upon reaching subconfluence. Passage 1 (P1) cells were seeded into six-well plates at a density of 2×10^5 cells/well. Two days after seeding, the cells were treated with carrier-free recombinant human NTN4 (1254-N4/CF; R&D Systems, Minneapolis, MN, USA) at 0, 50, or 500 ng/mL for 6 or 24 h, with one well per treatment condition in each independent experiment. Recombinant human NTN4 was used because the corresponding mouse recombinant protein had been discontinued and was unavailable. The recombinant protein was produced in mouse myeloma NS0 cells and supplied as a lyophilized preparation containing PBS and trehalose without carrier protein. The protein was reconstituted in sterile PBS, and an equivalent volume of PBS was added to the 0 ng/mL control group. According to the manufacturer's specifications, the endotoxin content was less than 1.0 EU/μg of protein. Endotoxin levels in the final treatment solutions were not independently measured. The NTN4 concentrations were selected based on those previously used in our in vitro studies involving human fibroblasts, human iPS-derived sensory neurons, and rat rotator cuff cells [21,23,24]. For Western blot analysis, separate wells were prepared in parallel using cells from the same four independent isolations under identical experi-

mental conditions. Proteins were extracted from these separate wells after 24 h of NTN4 treatment using an SDS-containing extraction buffer. NEO1 and UNC5B immunoreactive band intensities were normalized to GAPDH, and the normalized values were expressed relative to the mean of the 0 ng/mL NTN4 control group, which was set to 1. Western blotting was performed as described in Section 2.3.

Total RNA was extracted at each time point, and the expression of *Neo1*, *Unc5b*, *Acan*, *Col2a1*, *Mmp3*, *Mmp13*, *Il6*, and *Tnf* was analyzed by qPCR as described in Section 2.2. Culture supernatants were collected only at 24 h after treatment from the same wells used for qPCR analysis, before RNA extraction. MMP-3 concentrations were measured using the Mouse Total MMP-3 Quantikine ELISA Kit (MMP300; R&D Systems, Minneapolis, MN, USA), and MMP-13 concentrations were measured using the Mouse MMP13 ELISA Kit–Extracellular (ab316904; Abcam, Cambridge, UK). These assays measured immunoreactive MMP-3 and MMP-13 protein concentrations rather than their enzymatic activities. TNF-α and IL-6 concentrations were measured using the ELISA MAX Standard Set Mouse TNF-α (Cat. No. 430904; BioLegend, San Diego, CA, USA) and the LEGEND MAX Mouse IL-6 ELISA Kit (Cat. No. 431307; BioLegend), respectively, according to the manufacturers' instructions. For ELISA measurements, culture supernatants were analyzed either undiluted or after dilution with the appropriate assay diluent. IL-6 and TNF-α concentrations were measured using undiluted supernatants. For MMP-3 measurements, supernatants from the 0 and 50 ng/mL NTN4 groups were diluted 2-fold, whereas those from the 500 ng/mL group were diluted 20-fold. For MMP-13 measurements, supernatants from all treatment groups were diluted 40-fold. All quantifiable MMP-3, MMP-13, and IL-6 concentrations were within the respective assay standard curve ranges, whereas TNF-α concentrations were below the lowest concentration of the standard curve (7.8 pg/mL). The concentrations reported in this study were calculated by correcting for the corresponding dilution factors. All qPCR, ELISA, and Western blot analyses were based on the same four independent cell isolations, which were treated as biological replicates ($n = 4$). No technical replicate wells were averaged within each independent experiment. No additional mice or independent cell isolations were used for the Western blot analyses.

2.6. Statistical Analysis

Statistical analyses were performed using IBM SPSS Statistics, version 28.0.0.0 (IBM Corp., Armonk, NY, USA). Gene expression, ELISA, and Western blot data are presented as box-and-whisker plots, with boxes representing the interquartile range (25th–75th percentiles), horizontal lines indicating the median, and whiskers denoting the minimum and maximum values. Individual data points represent independent biological replicates. Normality of qPCR and Western blot data was assessed using the Shapiro–Wilk test.

Statistical analyses of qPCR data were performed using ΔCt values. For in vivo analyses, differences among the four independent groups were assessed using one-way ANOVA followed by Bonferroni-adjusted pairwise comparisons when parametric assumptions were considered appropriate. Otherwise, the Kruskal–Wallis test followed by Bonferroni-adjusted pairwise comparisons was used.

For in vitro analyses, the four independent cell isolations were treated as matched experimental units. Differences among NTN4 concentrations were assessed separately at 6 and 24 h using repeated-measures one-way ANOVA followed by Bonferroni-adjusted pairwise comparisons when parametric assumptions were considered appropriate. When sphericity was violated, the Greenhouse–Geisser correction was applied. When parametric assumptions were not met, the Friedman test followed by Bonferroni-adjusted pairwise comparisons was used.

For ELISA analyses, differences among the three treatment concentrations at 24 h were assessed using repeated-measures one-way ANOVA followed by Bonferroni-adjusted pairwise comparisons. The Greenhouse–Geisser correction was applied when the assumption of sphericity was violated.

For in vivo Western blot analysis, homogeneity of variances was evaluated using Levene's test. Differences between the two independent groups were assessed using Student's *t*-test when normality and homogeneity of variances were satisfied, or Welch's *t*-test when normality was satisfied but homogeneity of variances was not. For in vitro Western blot analysis, differences among the three NTN4 concentrations were assessed using repeated-measures one-way ANOVA followed by Bonferroni-adjusted pairwise comparisons for NEO1, and the Friedman test followed by Bonferroni-adjusted pairwise comparisons for UNC5B.

For cultured-cell receptor Western blotting, a supplementary descriptive comparison of the raw immunoreactive band intensities and the corresponding within-isolation target/GAPDH ratios was performed using the four existing cell isolations. Group means were used to describe percentage changes relative to 0 ng/mL; no additional inferential tests were performed on unnormalized band intensities.

p values < 0.05 were considered statistically significant. Bonferroni-adjusted p values were used for multiple pairwise comparisons, where applicable. For in vitro analyses, multiplicity correction was applied separately within each biomarker- and time point-specific family of pairwise comparisons among NTN4 concentrations, rather than across all biomarkers and time points.

3. Results

3.1. Ntn4 and Putative Receptor Expression and Anti-NTN4 Immunoreactivity Following Intervertebral Disc Injury

The expression of *Ntn4* and its putative receptors, *Neo1* and *Unc5b*, was examined at 0, 7, 14, and 28 days after IVD injury. *Ntn4* expression was significantly decreased at day 7 ($p = 0.013$), followed by significant increases at days 14 ($p = 0.014$) and 28 ($p < 0.001$) compared with day 0 (Figure 1A). Similarly, *Neo1* expression decreased at day 7 ($p = 0.003$), increased at day 14 ($p = 0.004$), and showed no significant difference at day 28 ($p = 1.000$; Figure 1B). *Unc5b* expression was significantly reduced at day 7 ($p = 0.024$), whereas no significant differences were observed at days 14 ($p = 0.149$) or 28 ($p = 1.000$; Figure 1C).

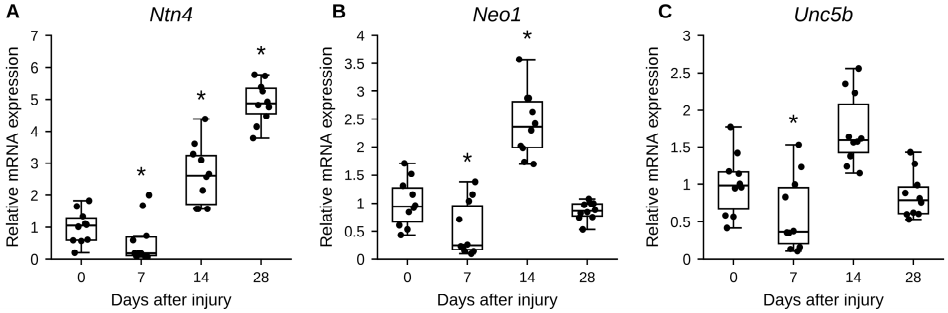


Figure 1. Temporal changes in *Ntn4*, *Neo1*, and *Unc5b* mRNA expression after intervertebral disc injury. Relative mRNA expression levels of (**A**) *Ntn4*, (**B**) *Neo1*, and (**C**) *Unc5b* were evaluated by quantitative real-time PCR at days 0, 7, 14, and 28 after disc injury ($n = 10$ per group). Day 0 served as the uninjured control. Boxes represent the interquartile range (25th–75th percentiles), horizontal lines indicate the median, and whiskers denote the minimum and maximum values. Individual dots represent data from individual mice ($n = 10$ per group). Statistical significance was assessed using one-way ANOVA followed by Bonferroni-adjusted multiple comparisons. * $p < 0.05$ versus day 0.

To examine changes in NTN4 and its receptors at the protein level following IVD injury, Western blotting was performed using antibodies against NTN4, NEO1, and UNC5B. The GAPDH-normalized intensity of the NTN4-immunoreactive band was 2.02-fold higher at day 14 after injury than in uninjured controls ($p = 0.001$, Welch's *t*-test; Figure 2A,B).

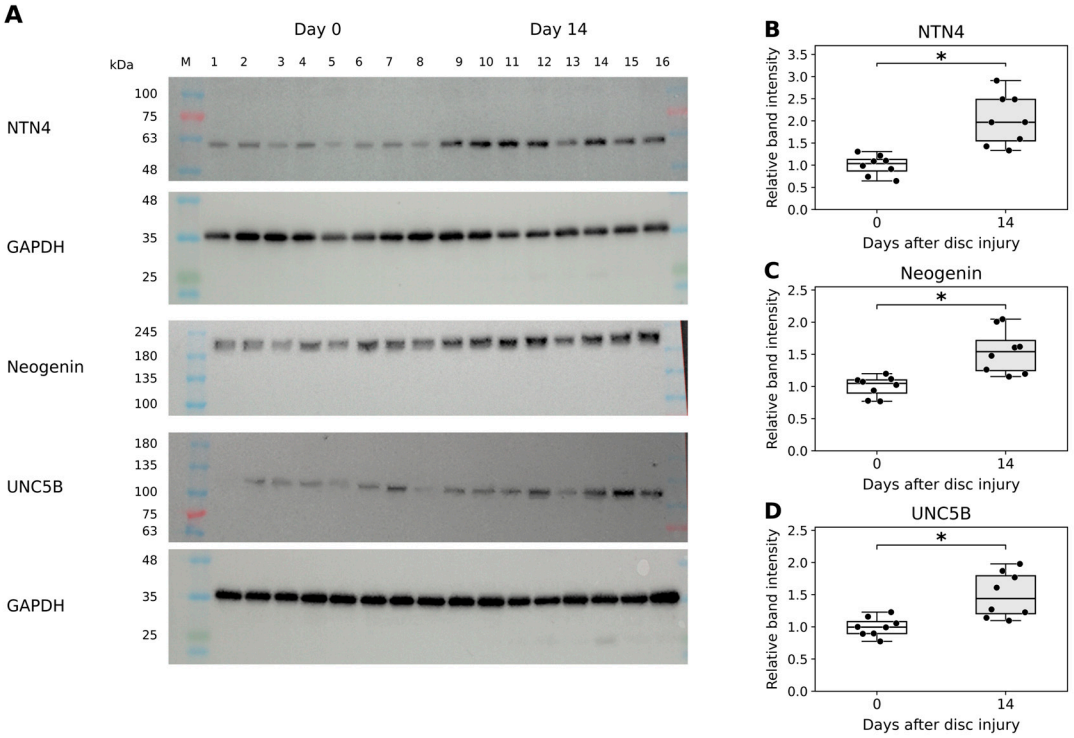


Figure 2. Increased NTN4-, Neogenin-, and UNC5B-related immunoreactivity after intervertebral disc injury. (**A**) Western blot analysis using antibodies against NTN4, Neogenin, UNC5B, and GAPDH. Molecular-weight markers are indicated in kilodaltons (kDa). M, molecular weight marker; lanes 1–8, uninjured controls (day 0); lanes 9–16, day 14 after disc injury. (**B**–**D**) Densitometric quantification of NTN4-immunoreactive (**B**), Neogenin-immunoreactive (**C**), and UNC5B-immunoreactive (**D**) band intensities. Band intensities were normalized to GAPDH and expressed relative to the mean of the day 0 control group. For NTN4 analysis, exposure times were 20 s for NTN4 and 10 s for the corresponding GAPDH loading control obtained from the same membrane. For receptor analysis, exposure times were 2 min 30 s for UNC5B, 15 s for Neogenin, and 5 s for the corresponding GAPDH loading control obtained from the receptor membrane. Boxes represent the interquartile range (25th–75th percentiles), horizontal lines indicate the median, and whiskers denote the minimum and maximum values. Individual dots represent data from individual mice ($n = 8$ per group). Statistical significance was assessed using Welch's *t*-test for NTN4 (**B**) and UNC5B (**D**), and Student's *t*-test for Neogenin (**C**). * $p < 0.05$ versus day 0.

Similarly, the GAPDH-normalized intensities of the NEO1- and UNC5B-immunoreactive bands were significantly higher at day 14 after injury, showing 1.55-fold ($p = 0.001$, Student's *t*-test; Figure 2A,C) and 1.50-fold ($p = 0.005$, Welch's *t*-test; Figure 2A,D) increases, respectively.

Uncropped Western blot images for NTN4, NEO1, and UNC5B are provided in Supplementary Figures S2 and S3, and the corresponding raw densitometric values are presented in Supplementary Table S2.

Immunohistochemical analysis revealed immunoreactivity detected using the anti-NTN4 antibody in cells located within the nucleus pulposus (NP) region at day 14 after injury (Figure 3). Immunoreactivity was also observed in adjacent marrow-associated

regions at both time points. No appreciable DAB staining was observed in the corresponding no-primary-antibody controls (Supplementary Figure S1).

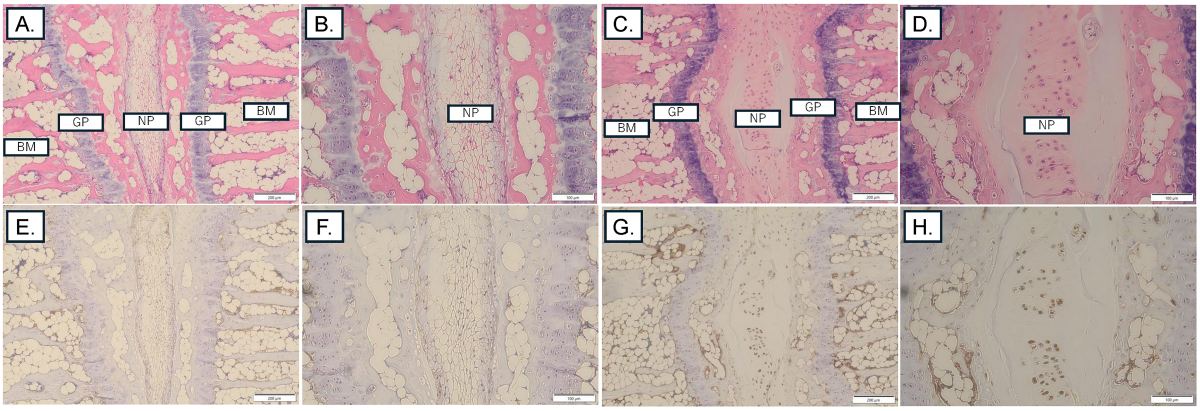


Figure 3. Histological changes and Netrin-4 (NTN4) immunoreactivity in mouse intervertebral discs before and after puncture injury. Representative hematoxylin and eosin (H&E)-stained sections and NTN4 immunohistochemical images of mouse intervertebral discs at baseline (day 0) and 14 days after puncture injury (day 14). H&E staining and NTN4 immunohistochemistry were performed on serial sections from the same intervertebral discs. (**A**,**B**) H&E staining at day 0 at low (**A**) and high (**B**) magnification. (**C**,**D**) H&E staining at day 14 at low (**C**) and high (**D**) magnification. (**E**,**F**) NTN4 immunohistochemical staining at day 0 at low (**E**) and high (**F**) magnification. (**G**,**H**) NTN4 immunohistochemical staining at day 14 at low (**G**) and high (**H**) magnification. NTN4 immunoreactivity was observed in cells located within the nucleus pulposus region at day 14. Anatomical regions are indicated in the H&E-stained images: NP, nucleus pulposus; GP, growth plate; BM, bone marrow. Corresponding no-primary-antibody controls are presented in Supplementary Figure S1. The images are representative of five mice per group, and no standardized blinded histological degeneration score was obtained. The observed morphological changes reflect the experimentally induced puncture injury model and should not be interpreted as evidence of progressive clinical intervertebral disc degeneration. Scale bars: 200 µm (**A**,**C**,**E**,**G**) and 100 µm (**B**,**D**,**F**,**H**).

3.2. Temporal Changes in Extracellular Matrix, MMP, and Inflammatory Cytokine Gene Expression Following Intervertebral Disc Injury

The expression of extracellular matrix-, MMP-, and inflammatory cytokine-related genes was also evaluated following IVD injury. *Acan* expression was significantly increased at days 7 ($p < 0.001$), 14 ($p < 0.001$), and 28 ($p = 0.009$) compared with day 0 (Figure 4A). *Col2a1* expression increased significantly at days 14 ($p = 0.003$) and 28 ($p = 0.005$), but not at day 7 ($p = 1.000$; Figure 4B). Among MMP-related genes, *Mmp3* expression was significantly elevated at days 14 ($p = 0.010$) and 28 ($p < 0.001$), whereas no significant difference was observed at day 7 ($p = 1.000$; Figure 4C). *Mmp13* expression increased significantly at day 14 ($p = 0.003$), but not at days 7 ($p = 1.000$) or 28 ($p = 0.648$; Figure 4D). Regarding inflammatory cytokine-related genes, *Il6* expression was significantly increased at days 14 ($p < 0.001$) and 28 ($p = 0.013$), but not at day 7 ($p = 1.000$; Figure 4E). *Tnf* expression increased significantly at day 14 ($p < 0.001$), whereas no significant differences were observed at days 7 ($p = 1.000$) or 28 ($p = 0.212$; Figure 4F).

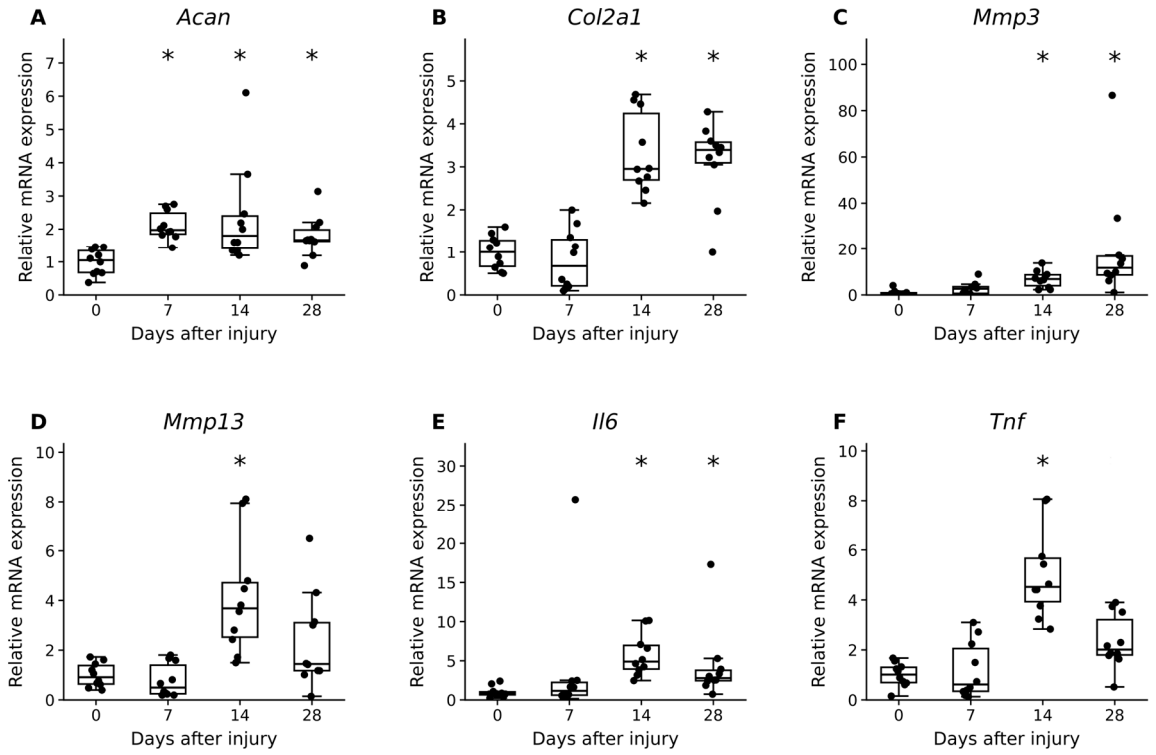


Figure 4. Temporal changes in extracellular matrix, MMP, and inflammatory cytokine gene expression following intervertebral disc injury. The relative mRNA expression levels of (**A**) *Acan*, (**B**) *Col2a1*, (**C**) *Mmp3*, (**D**) *Mmp13*, (**E**) *Il6*, and (**F**) *Tnf* were measured by qPCR in mouse intervertebral disc tissues at baseline (day 0) and on days 7, 14, and 28 after injury. Expression levels were normalized to *Gapdh* and expressed relative to the day 0 control group. Boxes represent the interquartile range (25th–75th percentiles), horizontal lines indicate the median, and whiskers represent the minimum and maximum values. Individual dots represent data from individual mice ($n = 10$ per group). Statistical comparisons were performed using one-way ANOVA followed by Bonferroni-adjusted multiple comparisons for *Acan*, *Mmp13*, and *Il6*, and the Kruskal–Wallis test followed by Bonferroni-adjusted pairwise comparisons for *Col2a1*, *Mmp3*, and *Tnf*. * $p < 0.05$ versus day 0.

3.3. Gene Expression and Protein Measurements Following Exposure to the Recombinant NTN4 Preparation in Cultured Mouse IVD Cells

Because *Ntn4* upregulation coincided temporally with changes in extracellular matrix, MMP, and inflammatory cytokine gene expression after IVD injury, we next examined cellular responses following exposure to the recombinant NTN4 preparation in cultured mouse IVD cells. Cells were treated with recombinant NTN4 at 0, 50, or 500 ng/mL, and gene expression was assessed after 6 and 24 h. All comparisons were made against the 0 ng/mL control group at the corresponding time point. At 6 h, repeated-measures ANOVA revealed no significant overall effect of recombinant NTN4 exposure on *Neo1* mRNA expression ($F(2, 6) = 2.617$, $p = 0.152$), with no significant differences at either 50 or 500 ng/mL (50 ng/mL, $p = 0.654$; 500 ng/mL, $p = 0.341$; Figure 5A). At 24 h, the overall effect was also not significant ($F(2, 6) = 2.828$, $p = 0.136$); however, an exploratory post hoc Bonferroni-adjusted pairwise comparison indicated significantly higher *Neo1* expression at 500 ng/mL compared with the control ($p = 0.047$), whereas no significant difference was observed at 50 ng/mL ($p = 1.000$). For *Unc5b* mRNA expression, no significant overall effects were observed at either 6 h ($F(2, 6) = 0.295$, $p = 0.755$) or 24 h ($F(2, 6) = 3.097$, $p = 0.119$). Bonferroni-adjusted pairwise comparisons revealed no significant differences at 6 h (50 ng/mL, $p = 1.000$; 500 ng/mL, $p = 1.000$) or 24 h (50 ng/mL, $p = 0.843$; 500 ng/mL, $p = 0.413$; Figure 5B). Western blot analysis revealed no significant overall difference in NEO1-immunoreactive band

intensity among the NTN4 treatment groups (repeated-measures ANOVA, $F(2, 6) = 2.520$, $p = 0.161$; Figure 5C,D). However, an exploratory post hoc Bonferroni-adjusted pairwise comparison indicated a lower GAPDH-normalized intensity at 50 ng/mL than at 0 ng/L ($p = 0.033$), whereas no significant difference was observed between the 0 and 500 ng/mL groups ($p = 1.000$; Figure 5C,D). In contrast, the Friedman test revealed a significant overall treatment effect on UNC5B-immunoreactive band intensity ($\chi^2(2) = 6.000$, $p = 0.0498$). However, neither Bonferroni-adjusted pairwise comparison with the control group reached statistical significance (50 ng/mL, $p = 0.102$; 500 ng/mL, $p = 0.102$; Figure 5C,E). These receptor-band comparisons depend on normalization to the corresponding GAPDH signals and should not be taken as evidence of altered receptor abundance or activation.

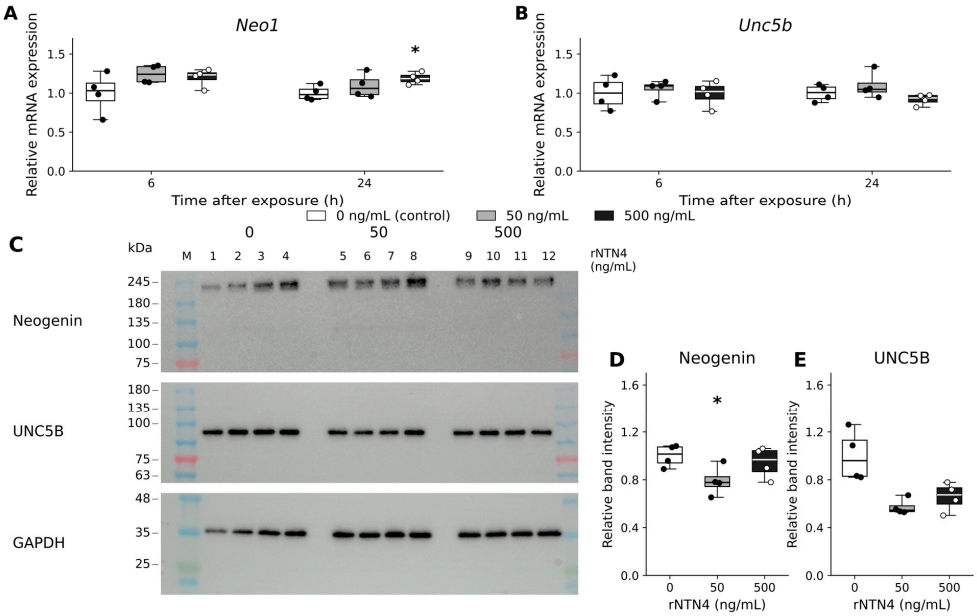


Figure 5. *Neo1* and *Unc5b* mRNA expression and NEO1- and UNC5B-immunoreactive band intensities following exposure to the recombinant NTN4 preparation in cultured mouse intervertebral disc cells. (**A**,**B**) Relative mRNA expression levels of *Neo1* (**A**) and *Unc5b* (**B**) in mouse intervertebral disc (IVD) cells following exposure to the recombinant NTN4 preparation (0, 50, or 500 ng/mL) for 6 or 24 h. (**C**) Representative Western blots showing immunoreactive bands detected using antibodies against NEO1 and UNC5B following 24 h of exposure to the recombinant NTN4 preparation, with GAPDH as a loading control. (**D**,**E**) Quantification of NEO1-immunoreactive (**D**) and UNC5B-immunoreactive (**E**) band intensities normalized to GAPDH. Raw densitometric values for NEO1, UNC5B, and the corresponding GAPDH loading controls are provided in Supplementary Table S4. Exposure times were 1 min 14 s for UNC5B, 1 min 18 s for Neogenin, and 15 s for the corresponding GAPDH loading control. Four independent cell isolations were performed ($n = 4$ biological replicates), each using pooled IVD cells obtained from 30 discs collected from five mice. Boxes represent the interquartile range (25th–75th percentiles), horizontal lines indicate the median, and whiskers denote the minimum and maximum values. Individual dots represent independent cell isolations. For qPCR analyses, differences among NTN4 concentrations were assessed separately at each time point using repeated-measures one-way ANOVA followed by Bonferroni-adjusted pairwise comparisons, or the Friedman test followed by Bonferroni-adjusted pairwise comparisons when parametric assumptions were not met. Western blot data were analyzed using repeated-measures one-way ANOVA followed by Bonferroni-adjusted pairwise comparisons for NEO1, and the Friedman test followed by Bonferroni-adjusted pairwise comparisons for UNC5B. * $p < 0.05$ versus the corresponding 0 ng/mL control.

To assess the sensitivity of these receptor-band comparisons to GAPDH normalization, we descriptively compared unnormalized and normalized densitometric values from the same four independent cell isolations (Supplementary Table S4). At

50 ng/mL relative to 0 ng/mL, mean unnormalized NEO1-immunoreactive band intensity was 6.9% higher, whereas the mean of the within-isolation NEO1/GAPDH ratios was 20.9% lower. For UNC5B, the corresponding differences were −17.2% and −42.8%, respectively. Mean unnormalized GAPDH intensity was 37.4% higher at 50 ng/mL than at 0 ng/mL. These comparisons were descriptive only; no inferential tests of unnormalized intensities were performed.

Uncropped Western blot images and the corresponding raw densitometric values for cultured IVD cells are provided in Supplementary Figure S4 and Supplementary Table S4, respectively.

Acan expression was not significantly altered among the NTN4 exposure groups at 6 h (repeated-measures ANOVA, $F(2, 6) = 3.037$, $p = 0.123$), with no significant differences following exposure to 50 or 500 ng/mL NTN4 ($p = 0.107$ and $p = 0.883$, respectively). At 24 h, a significant overall effect was observed ($F(2, 6) = 21.287$, $p = 0.002$). *Acan* expression was lower after exposure to 500 ng/mL of the recombinant NTN4 preparation ($p = 0.047$), whereas no significant change was observed with 50 ng/mL ($p = 0.205$; Figure 6A). No significant overall difference in *Col2a1* expression was observed among treatment groups at 6 h (Friedman test, $\chi^2(2) = 2.000$, $p = 0.368$). At 24 h, repeated-measures ANOVA revealed a significant overall effect ($F(2, 6) = 84.146$, $p < 0.001$). *Col2a1* expression was lower following exposure to 500 ng/mL of the recombinant NTN4 preparation ($p = 0.004$), whereas no significant difference was observed at 50 ng/mL ($p = 0.296$; Figure 6B). A significant overall effect on *Mmp3* expression was observed at 6 h ($F(2, 6) = 53.699$, $p < 0.001$). *Mmp3* expression was significantly higher following exposure to 500 ng/mL of the recombinant NTN4 preparation at 6 h ($p = 0.010$), whereas no significant difference was observed at 50 ng/mL. At 24 h, a significant overall effect was also detected (Greenhouse–Geisser-corrected repeated-measures ANOVA, $F(1.009, 3.026) = 1674.346$, $p < 0.001$), with significantly higher *Mmp3* expression at both 50 and 500 ng/mL than at 0 ng/mL ($p = 0.002$ and $p < 0.001$, respectively; Figure 6C). Repeated-measures ANOVA revealed significant overall effects on *Mmp13* expression at both 6 h ($F(2, 6) = 394.720$, $p < 0.001$) and 24 h ($F(2, 6) = 1354.685$, $p < 0.001$). *Mmp13* expression was higher following exposure to both 50 and 500 ng/mL of the recombinant NTN4 preparation at 6 h ($p = 0.013$ and $p < 0.001$, respectively), with similar effects at 24 h (both $p < 0.001$; Figure 6D). Significant overall effects on *Il6* expression were also observed at 6 h ($F(2, 6) = 777.312$, $p < 0.001$) and 24 h ($F(2, 6) = 328.407$, $p < 0.001$). *Il6* expression was also higher following exposure to both concentrations at 6 h ($p = 0.003$ and $p < 0.001$ for 50 and 500 ng/mL, respectively) and 24 h ($p = 0.011$ and $p < 0.001$, respectively; Figure 6E). A significant overall effect on *Tnf* expression was detected at 6 h (repeated-measures ANOVA, $F(2, 6) = 27.496$, $p < 0.001$) and at 24 h (Friedman test, $\chi^2(2) = 6.500$, $p = 0.039$).

Tnf expression was significantly higher following exposure to 500 ng/mL of the recombinant NTN4 preparation at both 6 h ($p = 0.009$) and 24 h ($p = 0.040$), whereas no significant differences were observed at 50 ng/mL at either time point ($p = 0.836$ and $p = 1.000$, respectively; Figure 6F).

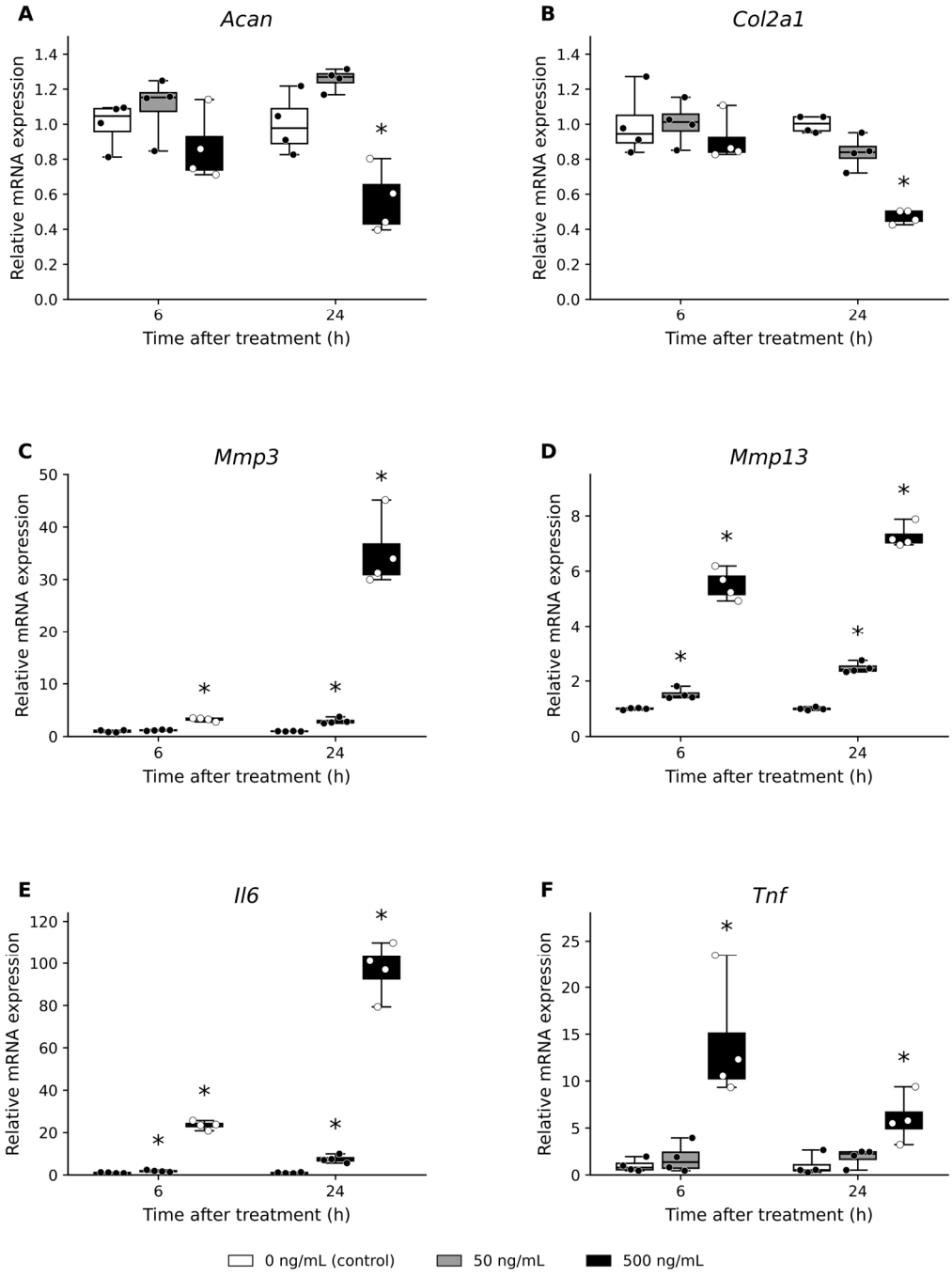


Figure 6. Extracellular matrix, matrix metalloproteinase, and inflammatory cytokine gene expression following exposure to the recombinant NTN4 preparation in intervertebral disc cells. Relative mRNA expression levels of (**A**) *Acan*, (**B**) *Col2a1*, (**C**) *Mmp3*, (**D**) *Mmp13*, (**E**) *Il6*, and (**F**) *Tnf* were evaluated by quantitative real-time PCR following treatment with NTN4 (0, 50, or 500 ng/mL) for 6 or 24 h. Four independent cell isolations were performed ($n = 4$ biological replicates), each using pooled intervertebral disc cells obtained from 30 discs collected from five mice. White, gray, and black boxes indicate 0 (control), 50, and 500 ng/mL NTN4, respectively. Boxes represent the interquartile range (25th–75th percentiles), horizontal lines indicate the median, and whiskers denote the minimum and maximum values. Individual dots represent independent cell isolations. Statistical significance was assessed using repeated-measures one-way ANOVA followed by Bonferroni-adjusted pairwise comparisons, except for *Col2a1* at 6 h and *Tnf* at 24 h, which were analyzed using the Friedman test followed by Bonferroni-adjusted pairwise comparisons. * $p < 0.05$ versus the corresponding 0 ng/mL control at the same time point.

ELISA analysis of culture supernatants collected after 24 h showed significant concentration-group differences in MMP-3 (Greenhouse–Geisser-corrected repeated-measures ANOVA, $F(1.002, 3.007) = 28.735$, $p = 0.013$), MMP-13 (repeated-measures ANOVA, $F(2, 6) = 106.856$, $p < 0.001$), and IL-6 protein (Greenhouse–Geisser-corrected repeated-measures ANOVA, $F(1.009, 3.026) = 232.117$, $p < 0.001$) concentrations (Figure 7A–C). Bonferroni-adjusted pairwise comparisons showed that MMP-3 ($p = 0.035$), MMP-13 ($p = 0.002$), and IL-6 ($p = 0.002$) concentrations were higher following exposure to 500 ng/mL of the recombinant NTN4 preparation compared with the 0 ng/mL control. At 50 ng/mL, IL-6 concentrations were higher than in controls ($p = 0.014$), whereas no significant differences were observed in MMP-3 ($p = 0.090$) or MMP-13 ($p = 0.066$) concentrations compared with the control. TNF-α concentrations were below the lowest concentration of the standard curve used in this study (7.8 pg/mL) in all treatment groups.

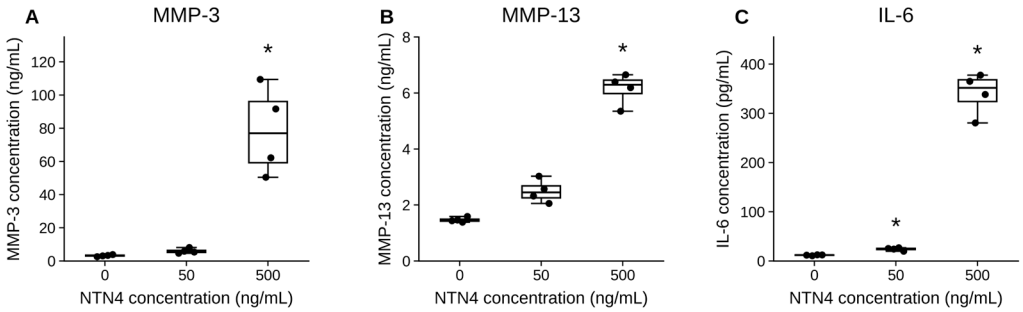


Figure 7. MMP-3, MMP-13, and IL-6 concentrations in intervertebral disc cell culture supernatants following exposure to the recombinant NTN4 preparation. Concentrations of (**A**) MMP-3, (**B**) MMP-13, and (**C**) IL-6 in culture supernatants were measured by ELISA 24 h after treatment of intervertebral disc cells with recombinant NTN4 (0, 50, or 500 ng/mL). Four independent cell isolations were performed ($n = 4$ biological replicates), each using pooled intervertebral disc cells obtained from 30 discs collected from five mice. Boxes represent the interquartile range (25th–75th percentiles), horizontal lines indicate the median, and whiskers denote the minimum and maximum values. Individual dots represent independent cell isolations. Statistical significance was assessed using repeated-measures one-way ANOVA followed by Bonferroni-adjusted pairwise comparisons. The Greenhouse–Geisser correction was applied when the assumption of sphericity was violated. * $p < 0.05$ versus the corresponding 0 ng/mL control.

Individual dilution-corrected ELISA concentrations for each independent cell isolation are provided in Supplementary Table S5. Exploratory paired exposure-to-control ratios and their unadjusted 95% confidence intervals for the in vitro qPCR, Western blot, and ELISA analyses are provided in Supplementary Table S6.

4. Discussion

The present study demonstrated that *Ntn4* expression increased at days 14 and 28 after IVD injury in mice, whereas *Neo1* expression increased at day 14 and *Unc5b* expression did not differ significantly from baseline at this time point. Western blotting showed an increased intensity of an approximately 63 kDa immunoreactive band detected using an anti-NTN4 antibody at day 14 after injury. Immunohistochemistry demonstrated NTN4 immunoreactivity in cells located within the nucleus pulposus region. In cultured mouse IVD cells, recombinant NTN4 exposure was associated with increased inflammatory cytokine and MMP gene expression, increased IL-6, MMP-3, and MMP-13 concentrations in culture supernatants, and reduced *Acan* and *Col2a1* expression. These findings indicate that *Ntn4* expression increases following IVD injury and that exposure to the tested recom-

binant NTN4 preparation is associated with inflammatory and matrix-related responses in cultured IVD cells.

The onset of *Ntn4* upregulation coincided with the reported emergence of *Col2a1*-expressing chondrocyte-like cells beginning approximately 14 days after puncture injury [27]. In the present study, *Col2a1* expression increased at days 14 and 28, whereas *Acan* expression was elevated from day 7 through day 28. These changes may reflect an endogenous matrix-repair response following injury. The detection of NTN4 immunoreactivity in cells located within the NP region at day 14 is consistent with a possible association between NTN4 distribution and injury-associated cellular changes. However, the cellular source of NTN4 remains undetermined. NTN4 expression has also been reported to increase after rotator cuff injury, with TNF-α proposed as a potential regulator [21]. In osteoarthritis-related tissues, NTN4 has been associated with stromal cell activation, inflammatory changes, and sensory neuron-related responses [23,24]. The present findings extend these observations to the IVD and suggest that NTN4 may be an injury-responsive molecule in musculoskeletal tissues.

TNF-α and IL-6 are established mediators of IVD degeneration and promote inflammatory responses and matrix-degrading pathways in disc cells [7,8]. The higher IL-6 concentration in culture supernatants was consistent with the observed gene-expression response, although the present design does not establish a direct mechanistic link. In contrast, *Tnf* induction was not accompanied by quantifiable TNF-α concentrations in culture supernatants at 24 h, suggesting differential regulation of these cytokines following exposure to the recombinant NTN4 preparation. This discrepancy may reflect post-transcriptional regulation or differences in the timing of mRNA expression and protein secretion. Because TNF-α protein concentrations were assessed only at 24 h, transient secretion at earlier time points cannot be excluded. Additional measurements at earlier time points are needed to clarify this discrepancy. These findings indicate that recombinant NTN4 exposure was associated with inflammatory responses in cultured IVD cells. However, they do not establish NTN4-specific activity or a causal contribution of endogenous NTN4 to post-injury inflammation.

Type II collagen forms an important part of the collagenous framework of the IVD matrix, whereas aggrecan contributes to tissue hydration and resistance to compressive loading [2,28,29]. In the present injury model, the earlier increase in *Acan* expression followed by the elevation in *Col2a1* may reflect activation of an endogenous matrix-repair response. Against this background, the matrix-related gene expression changes observed following recombinant NTN4 exposure are particularly relevant. Following exposure to the tested recombinant NTN4 preparation, cultured IVD cells showed higher *Mmp3* and *Mmp13* expression and lower *Acan* and *Col2a1* expression. MMP-3 and MMP-13 participate in proteoglycan and collagen degradation and have been implicated in ECM catabolism during IVD degeneration [9–11]. The increases in *Mmp3* and *Mmp13* expression, together with the reduction in *Col2a1* expression, suggest that recombinant NTN4 exposure is associated with a molecular profile characterized by increased expression of matrix-degrading enzymes and reduced expression of a matrix-related gene. These findings indicate that exposure to recombinant NTN4 is associated with increased expression of MMP-related genes and reduced expression of *Col2a1* in cultured IVD cells. However, whether endogenous NTN4 contributes to matrix degradation or interferes with repair processes following IVD injury remains unclear.

Immunohistochemistry revealed NTN4 immunoreactivity in cells located within the NP region following IVD injury. However, immunoreactivity does not establish that these cells synthesize NTN4 or that NTN4 acts through an autocrine or paracrine mechanism. Previous studies have implicated NEO1 and UNC5B in NTN4-mediated signaling in other

tissues [13,18–20]. In the present study, a post hoc Bonferroni-adjusted pairwise comparison suggested higher *Neo1* mRNA expression at 500 ng/mL after 24 h ($p = 0.047$), although the overall treatment effect was not statistically significant ($p = 0.136$). Similarly, a post hoc Bonferroni-adjusted pairwise comparison indicated lower GAPDH-normalized NEO1-immunoreactive band intensity at 50 ng/mL than at 0 ng/mL ($p = 0.033$), whereas the overall treatment effect was not statistically significant ($p = 0.161$). These post hoc pairwise findings should be interpreted as exploratory given the nonsignificant omnibus tests, four independent cell isolations, and multiple biomarkers examined.

Comparison of raw and normalized densitometric values showed that the mean NEO1-immunoreactive band intensity at 50 ng/mL was 6.9% higher before normalization but 20.9% lower after GAPDH normalization. For UNC5B, the corresponding differences at 50 ng/mL relative to 0 ng/mL were decreases of 17.2% and 42.8%, respectively. These findings indicate that the receptor-band comparisons were sensitive to GAPDH normalization, although the source of the GAPDH signal variation remains unknown. Confirmation using independently validated normalization methods would be needed before drawing conclusions about receptor abundance.

In vivo, *Unc5b* mRNA expression did not differ significantly from baseline at day 14, whereas UNC5B-immunoreactive band intensity was significantly higher after injury. This discrepancy may reflect differences between transcript-level and antibody-based measurements; however, the underlying mechanisms remain unclear. These observations do not establish changes in receptor protein abundance or receptor activation. Whether NEO1 or UNC5B contributes to the observed inflammatory and matrix-related responses following exposure to the recombinant NTN4 preparation remains unclear and requires further investigation using receptor-specific loss- and gain-of-function approaches.

Importantly, the temporal expression patterns of *Ntn4* and inflammatory and matrix-related genes did not consistently correspond in vivo. Although *Ntn4* expression remained elevated at day 28, *Il6*, *Tnf*, and *Mmp13* expression decreased relative to day 14, whereas *Mmp3* remained elevated. Furthermore, *Acan* and *Col2a1* expression increased after injury, whereas both genes showed reduced expression following exposure to 500 ng/mL of the recombinant NTN4 preparation for 24 h in cultured IVD cells. These discrepancies suggest that NTN4 upregulation does not necessarily correspond to sustained inflammatory or catabolic responses in vivo. Several explanations are possible, including injury-associated chondroid changes, alterations in the cellular composition of IVD tissues, and secondary induction of NTN4 by inflammatory mediators such as TNF-α or IL-1β. In our previous study using a rat rotator cuff injury model, TNF-α was proposed as a potential regulator of *Ntn4* expression [21]. Therefore, increased NTN4 expression after IVD injury may reflect a downstream response to tissue injury rather than a direct driver of progressive matrix degradation. In addition, *Ntn4*, *Neo1*, and *Unc5b* expression levels were significantly decreased at day 7 compared with baseline. The biological significance of these early reductions remains unclear. Further studies are required to distinguish the potential roles of NTN4 in injury-associated inflammation, cellular remodeling, and matrix-related responses.

Several limitations should be acknowledged. First, although the growth plate and cartilaginous endplate were excluded from the tissues used for molecular analyses, age-related maturation of the nucleus pulposus and annulus fibrosus may have influenced gene expression during the observation period. Because age-matched uninjured or sham-operated controls were not included at each time point, these potential effects cannot be distinguished from those associated with disc injury. In addition, the amplification efficiencies of the qPCR primer pairs and the stability of *Gapdh* expression across experimental conditions were not independently validated, which may have affected the accuracy of relative gene expression measurements.

Second, the nucleus pulposus and annulus fibrosus were analyzed together, preventing compartment-specific evaluation of gene expression. Although immunoreactivity was observed in cells located within the NP region using an anti-NTN4 antibody, immunohistochemical staining alone cannot establish whether these cells synthesize NTN4. Further studies using cell-specific markers or spatial gene expression analyses are required to identify the cellular source of NTN4 and clarify its potential autocrine or paracrine actions. Third, anti-NTN4 immunoreactive band intensity and tissue immunoreactivity were examined only in uninjured controls (day 0) and at day 14, and their temporal profiles remain unknown. In addition, because immunohistochemical staining of day-0 and day-14 specimens was performed in separate runs, differences in staining intensity or the proportion of immunoreactive cells between the two time points could not be reliably assessed. Furthermore, the absence of antigen-specific controls prevents definitive confirmation of the specificity of the observed immunoreactivity. Although an approximately 63 kDa immunoreactive band was detected using an anti-NTN4 antibody, its molecular identity was not independently confirmed. Notably, a band at a similar apparent molecular weight is also observed in the manufacturer's representative Western blot image using mouse tissues, despite the predicted molecular weight of approximately 70 kDa. This discrepancy may reflect post-translational processing, including signal peptide cleavage. However, non-specific immunoreactivity cannot be excluded, particularly given the presence of additional immunoreactive bands. Similarly, although immunoreactive bands were detected at plausible molecular weights using antibodies against NEO1 and UNC5B, their molecular identities were not independently confirmed, and receptor-dependent signaling was not directly assessed. Further validation using independent approaches is required to confirm the identities of these immunoreactive bands. In addition, the efficacy of antibody stripping between sequential Western blot probing for UNC5B, NEO1, and GAPDH was not independently verified. Therefore, potential interference from residual antibodies cannot be completely excluded. Fourth, the cultured IVD cells were obtained from pooled NP and annulus fibrosus (AF) tissues and expanded in monolayer culture before stimulation. Although P1 cells were used, the relative proportions of NP- and AF-derived cells were not determined, and cell-type-specific marker expression was not evaluated at the time of treatment. Therefore, potential changes in cellular composition and phenotype during culture cannot be excluded, and the observed responses to recombinant NTN4 cannot be attributed to a specific IVD cell subtype. Fifth, the ELISA assays quantified MMP-3 and MMP-13 protein concentrations in culture supernatants but did not assess their enzymatic activities. Therefore, increased MMP protein concentrations do not necessarily indicate enhanced extracellular matrix proteolysis. Furthermore, secreted protein concentrations were not normalized to viable cell number or total cellular protein, and potential differences in cell number or viability among treatment groups may have influenced the measured concentrations. Sixth, the effective NTN4 concentration used in vitro may not reflect its local concentration in injured IVD tissue, which was not determined. In addition, recombinant human NTN4 was used to stimulate mouse IVD cells, and species-related differences in biological activity cannot be excluded. Endotoxin concentrations in the final treatment solutions were not independently measured, and the vehicle was not completely matched to the recombinant protein formulation because trehalose was absent from the control. Moreover, independent controls to exclude endotoxin- or preparation-associated effects and cell viability assays were not performed. Therefore, the observed inflammatory and matrix-related responses cannot be attributed specifically to NTN4 itself and should be interpreted as responses following exposure to the tested recombinant NTN4 product under the present culture conditions. Further experiments using formulation-matched vehicle controls, endotoxin-related controls, and cell viability assessments are necessary to establish

NTN4-specific biological activity. Seventh, the in vitro experiments were based on four independent cell isolations, limiting statistical power and the ability to assess distributional assumptions. Multiple genes and proteins were evaluated across different concentrations and time points, and multiplicity correction was applied within individual comparison families rather than across all biomarkers and time points. Therefore, findings with p values close to 0.05 should be interpreted as exploratory and require confirmation in larger independent experiments. For the ELISA analyses, although the Greenhouse–Geisser correction was applied to address violations of sphericity, it does not account for potential skewness or heterogeneity of variance in the concentration data. No log-transformed sensitivity analysis was performed. Therefore, the ELISA findings, particularly borderline pairwise comparisons, should be interpreted cautiously given the small number of independent cell isolations ($n = 4$). Finally, the functional experiments in this study were limited to gain-of-function approaches using exogenous recombinant NTN4. Neither loss-of-function experiments targeting endogenous NTN4 nor receptor-blocking experiments were performed. Therefore, whether endogenous NTN4 is necessary for inflammatory and catabolic responses following IVD injury remains unclear. Furthermore, the effects of NTN4 manipulation on disc structure and biomechanical function were not examined, limiting conclusions regarding its causal contribution to IVD degeneration in vivo. Further studies incorporating loss-of-function approaches and structural and biomechanical assessments are required to clarify the role of endogenous NTN4 in IVD degeneration. Because this study used only young male mice and a mouse coccygeal puncture model, the findings should also be interpreted with caution when extrapolating them to female or older animals and human lumbar IVD degeneration, where anatomy, loading environment, and disease progression differ. Sex- and age-dependent differences in inflammatory and matrix remodeling responses may further limit the generalizability of these findings.

5. Conclusions

Ntn4 mRNA expression and NTN4-immunoreactive band intensity increased following IVD injury. NTN4 immunoreactivity was observed in cells within the nucleus pulposus region of injured discs. Exposure to the tested recombinant NTN4 preparation was associated with increased expression of inflammatory cytokine- and matrix metalloproteinase-related genes and decreased expression of *Acan* and *Col2a1* in cultured IVD cells. However, these findings do not establish a causal role for endogenous NTN4 in inflammatory or catabolic responses following IVD injury. Further studies incorporating protein-specificity validation, loss-of-function approaches, and receptor-specific analyses are required to clarify the biological role of NTN4 in IVD injury.

Supplementary Materials: The following supporting information can be downloaded at https://www.mdpi.com/article/10.3390/biomedicines14112672/s1, Figure S1: Negative controls for Netrin-4 (NTN4) immunohistochemical staining in mouse intervertebral discs. Figure S2: Uncropped Western blot images showing NTN4-immunoreactive bands and the corresponding GAPDH loading control in mouse intervertebral disc tissues. Figure S3: Uncropped Western blot images showing NEO1- and UNC5B-immunoreactive bands and the corresponding GAPDH loading control in mouse intervertebral disc tissues. Figure S4: Uncropped Western blot images showing NEO1- and UNC5B-immunoreactive bands and the corresponding GAPDH loading control in cultured mouse intervertebral disc cells. Table S1: Raw quantification cycle (Cq) values of gene expression in mouse intervertebral disc tissues following injury. Table S2: Raw Western blot densitometric values of NTN4, NEO1, UNC5B, and their corresponding GAPDH loading controls in mouse intervertebral disc tissues before and after injury. Table S3: Raw quantification cycle (Cq) values of gene expression in cultured mouse intervertebral disc cells following recombinant NTN4 exposure. Table S4: Raw Western blot densitometric values of NEO1, UNC5B, and their corresponding GAPDH loading controls in

cultured mouse intervertebral disc cells following exposure to recombinant NTN4. Table S5: Dilution-corrected concentrations of MMP-3, MMP-13, and IL-6 in culture supernatants of mouse intervertebral disc cells following exposure to recombinant NTN4. Table S6: Estimated treatment effects and 95% confidence intervals.

Author Contributions: Conceptualization, K.U. and M.M.; methodology, K.U. and M.M.; validation, G.I., Y.U. and M.T.; formal analysis, N.S., Y.M. and Y.Y.; investigation, N.S. and Y.J.; data curation, Y.U.; writing—original draft preparation, N.S. and K.U.; writing—review and editing, M.M., G.I. and M.T.; visualization, N.S. and K.U.; supervision, G.I.; project administration, K.U. and M.M.; funding acquisition, Y.Y. and M.M. All authors have read and agreed to the published version of the manuscript.

Funding: This research was funded by the Grant-in-Aid for Scientific Research (C) (General), grant number 26K12088, the Grant-in-Aid for Early-Career Scientists, grant number 26K19883, Kitasato University Research Grant for Young Researchers, and the Parents' Association of Kitasato University School of Medicine. The funders had no role in the study design, data collection, analysis, interpretation, or manuscript preparation.

Institutional Review Board Statement: The animal study protocol was approved by the Kitasato University Animal Ethics Committee (protocol code 2026-006; date of approval: 1 June 2026).

Informed Consent Statement: Not applicable.

Data Availability Statement: The original contributions presented in this study are included in the article/Supplementary Material.

Acknowledgments: During the preparation of this manuscript, the authors used ChatGPT (OpenAI, GPT-5.5) to assist with English language editing. The authors reviewed and edited the output and take full responsibility for the content of this publication.

Conflicts of Interest: The authors declare no conflicts of interest.

Abbreviations

The following abbreviations are used in this manuscript:

NTN4	Netrin-4
DCC	deleted in colorectal cancer
UNC5B	Unc-5 netrin receptor B
ELISA	enzyme-linked immunosorbent assay
H&E	hematoxylin and eosin
DAB	3,3′-diaminobenzidine
NP	nucleus pulposus
AF	annulus fibrosus
IVD	Intervertebral disc
ECM	Extracellular matrix
TNF-α	tumor necrosis factor-alpha
IL-1β	interleukin-1β
IL-6	interleukin-6
MMP	Matrix metalloproteinase
NEO1	neogenin
qPCR	quantitative polymerase chain reaction
SDS	sodium dodecyl sulfate

References

1. Hartvigsen, J.; Hancock, M.J.; Kongsted, A.; Louw, Q.; Ferreira, M.L.; Genevay, S.; Hoy, D.; Karppinen, J.; Pransky, G.; Sieper, J.; et al. What low back pain is and why we need to pay attention. *Lancet* **2018**, *391*, 2356–2367. [CrossRef] [PubMed]
2. Chan, W.C.; Sze, K.L.; Samartzis, D.; Leung, V.Y.; Chan, D. Structure and biology of the intervertebral disk in health and disease. *Orthop. Clin. N. Am.* **2011**, *42*, 447–464. [CrossRef] [PubMed]
3. Raj, P.P. Intervertebral disc: Anatomy-physiology-pathophysiology-treatment. *Pain. Pract.* **2008**, *8*, 18–44. [CrossRef] [PubMed]

4. Adams, M.A.; Roughley, P.J. What is intervertebral disc degeneration, and what causes it? *Spine* **2006**, *31*, 2151–2161. [CrossRef] [PubMed]
5. Urban, J.P.; Roberts, S. Degeneration of the intervertebral disc. *Arthritis Res. Ther.* **2003**, *5*, 120–130. [CrossRef] [PubMed]
6. Martin, J.T.; Gorth, D.J.; Beattie, E.E.; Harfe, B.D.; Smith, L.J.; Elliott, D.M. Needle puncture injury causes acute and long-term mechanical deficiency in a mouse model of intervertebral disc degeneration. *J. Orthop. Res.* **2013**, *31*, 1276–1282. [CrossRef] [PubMed]
7. Johnson, Z.I.; Schoepflin, Z.R.; Choi, H.; Shapiro, I.M.; Risbud, M.V. Disc in flames: Roles of TNF-alpha and IL-1beta in intervertebral disc degeneration. *Eur. Cell Mater.* **2015**, *30*, 104–116; discussion 116–117. [CrossRef] [PubMed]
8. Risbud, M.V.; Shapiro, I.M. Role of cytokines in intervertebral disc degeneration: Pain and disc content. *Nat. Rev. Rheumatol.* **2014**, *10*, 44–56. [CrossRef] [PubMed]
9. Le Maitre, C.L.; Pockert, A.; Buttle, D.J.; Freemont, A.J.; Hoyland, J.A. Matrix synthesis and degradation in human intervertebral disc degeneration. *Biochem. Soc. Trans.* **2007**, *35*, 652–655. [CrossRef] [PubMed]
10. Vo, N.V.; Hartman, R.A.; Yurube, T.; Jacobs, L.J.; Sowa, G.A.; Kang, J.D. Expression and regulation of metalloproteinases and their inhibitors in intervertebral disc aging and degeneration. *Spine J.* **2013**, *13*, 331–341. [CrossRef] [PubMed]
11. Wang, W.J.; Yu, X.H.; Wang, C.; Yang, W.; He, W.S.; Zhang, S.J.; Yan, Y.G.; Zhang, J. MMPs and ADAMTSs in intervertebral disc degeneration. *Clin. Chim. Acta* **2015**, *448*, 238–246. [CrossRef] [PubMed]
12. Serafini, T.; Kennedy, T.E.; Galko, M.J.; Mirzayan, C.; Jessell, T.M.; Tessier-Lavigne, M. The netrins define a family of axon outgrowth-promoting proteins homologous to C. elegans UNC-6. *Cell* **1994**, *78*, 409–424. [CrossRef] [PubMed]
13. Dong, F.; Liu, Y.; Yan, W.; Meng, Q.; Song, X.; Cheng, B.; Yao, R. Netrin-4: Focus on Its Role in Axon Guidance, Tissue Stability, Angiogenesis and Tumors. *Cell Mol. Neurobiol.* **2023**, *43*, 1663–1683. [CrossRef] [PubMed]
14. Shu, F.; Huang, H.; Xiao, S.; Xia, Z.; Zheng, Y. Netrin-1 co-cross-linked hydrogel accelerates diabetic wound healing in situ by modulating macrophage heterogeneity and promoting angiogenesis. *Bioact. Mater.* **2024**, *39*, 302–316. [CrossRef] [PubMed]
15. Yagami, K.; Sadaoka, S.; Nakamura, M.; Nakamura, H.; Maki, S.; Yagasaki, T.; Udagawa, N. Neural-inducing factor Netrin-1 is regulated in chondrogenesis and osteogenesis by BMP or Noggin. *J. Hard Tissue Biol.* **2012**, *21*, 141–150. [CrossRef]
16. Ni, S.; Ling, Z.; Wang, X.; Cao, Y.; Wu, T.; Deng, R.; Crane, J.L.; Skolasky, R.; Demehri, S.; Zhen, G.; et al. Sensory innervation in porous endplates by Netrin-1 from osteoclasts mediates PGE2-induced spinal hypersensitivity in mice. *Nat. Commun.* **2019**, *10*, 5643. [CrossRef] [PubMed]
17. Zheng, B.; Li, S.; Xiang, Y.; Zong, W.; Ma, Q.; Wang, S.; Wu, H.; Song, H.; Ren, H.; Chen, J.; et al. Netrin-1 mediates nerve innervation and angiogenesis leading to discogenic pain. *J. Orthop. Transl.* **2023**, *39*, 21–33. [CrossRef] [PubMed]
18. Reuten, R.; Patel, T.R.; McDougall, M.; Rama, N.; Nikodemus, D.; Gibert, B.; Delcros, J.G.; Prein, C.; Meier, M.; Metzger, S.; et al. Structural decoding of netrin-4 reveals a regulatory function towards mature basement membranes. *Nat. Commun.* **2016**, *7*, 13515. [CrossRef] [PubMed]
19. Schneiders, F.I.; Maertens, B.; Bose, K.; Li, Y.; Brunken, W.J.; Paulsson, M.; Smyth, N.; Koch, M. Binding of netrin-4 to laminin short arms regulates basement membrane assembly. *J. Biol. Chem.* **2007**, *282*, 23750–23758. [CrossRef] [PubMed]
20. Lejmi, E.; Leconte, L.; Pedron-Mazoyer, S.; Ropert, S.; Raoul, W.; Lavalette, S.; Bouras, I.; Feron, J.G.; Maitre-Boube, M.; Assayag, F.; et al. Netrin-4 inhibits angiogenesis via binding to neogenin and recruitment of Unc5B. *Proc. Natl. Acad. Sci. USA* **2008**, *105*, 12491–12496. [CrossRef] [PubMed]
21. Inoue, K.; Uchida, K.; Tazawa, R.; Matsumoto, M.; Kenmoku, T.; Uekusa, Y.; Takaso, M. Elevation of NTN4 Expression and Its Possible Regulation by Tumor Necrosis Factor-Alpha (TNF-alpha) in a Rat Model of Rotator Cuff Tear. *Cureus* **2025**, *17*, e86324. [CrossRef] [PubMed]
22. Xiao, C.; Lara-Newman, D.; Zhou, Q.; Rosenblatt, M.I.; Guaiquil, V.H. Netrin-4 Modulates Corneal Wound Healing by Enhancing Corneal Epithelium and Nerve Regeneration. *FASEB BioAdv.* **2025**, *7*, e70021. [CrossRef] [PubMed]
23. Tsukada, A.; Uekusa, Y.; Ohta, E.; Hattori, A.; Mukai, M.; Iwase, D.; Aikawa, J.; Ohashi, Y.; Inoue, G.; Takaso, M.; et al. Association Between Synovial NTN4 Expression and Pain Scores, and Its Effects on Fibroblasts and Sensory Neurons in End-Stage Knee Osteoarthritis. *Cells* **2025**, *14*, 395. [CrossRef] [PubMed]
24. Uekusa, Y.; Mukai, M.; Tsukada, A.; Iwase, D.; Aikawa, J.; Shibata, N.; Ohashi, Y.; Inoue, G.; Takaso, M.; Uchida, K. Elevated Netrin-4 Expression and Its Action in Infrapatellar Fat Pad. *Int. J. Mol. Sci.* **2024**, *25*, 11369. [CrossRef] [PubMed]
25. Kawakubo, A.; Miyagi, M.; Yokozeki, Y.; Nakawaki, M.; Takano, S.; Satoh, M.; Itakura, M.; Inoue, G.; Takaso, M.; Uchida, K. Origin of M2 Mvarphi and its macrophage polarization by TGF-beta in a mice intervertebral injury model. *Int. J. Immunopathol. Pharmacol.* **2022**, *36*, 3946320221103792. [CrossRef] [PubMed]
26. Yokozeki, Y.; Kawakubo, A.; Miyagi, M.; Kuroda, A.; Sekiguchi, H.; Inoue, G.; Takaso, M.; Uchida, K. Reduced TGF-beta Expression and CD206-Positive Resident Macrophages in the Intervertebral Discs of Aged Mice. *BioMed Res. Int.* **2021**, *2021*, 7988320. [CrossRef] [PubMed]
27. Yang, F.; Leung, V.Y.; Luk, K.D.; Chan, D.; Cheung, K.M. Injury-induced sequential transformation of notochordal nucleus pulposus to chondrogenic and fibrocartilaginous phenotype in the mouse. *J. Pathol.* **2009**, *218*, 113–121. [CrossRef] [PubMed]

28. Hickman, T.T.; Rathan-Kumar, S.; Peck, S.H. Development, Pathogenesis, and Regeneration of the Intervertebral Disc: Current and Future Insights Spanning Traditional to Omics Methods. *Front. Cell Dev. Biol.* **2022**, *10*, 841831. [CrossRef] [PubMed]
29. Cherif, H.; Mannarino, M.; Pacis, A.S.; Ragoussis, J.; Rabau, O.; Ouellet, J.A.; Haglund, L. Single-Cell RNA-Seq Analysis of Cells from Degenerating and Non-Degenerating Intervertebral Discs from the Same Individual Reveals New Biomarkers for Intervertebral Disc Degeneration. *Int. J. Mol. Sci.* **2022**, *23*, 3993. [CrossRef] [PubMed]

Disclaimer/Publisher's Note: The statements, opinions and data contained in all publications are solely those of the individual author(s) and contributor(s) and not of MDPI and/or the editor(s). MDPI and/or the editor(s) disclaim responsibility for any injury to people or property resulting from any ideas, methods, instructions or products referred to in the content.